Contribution from the Laboratoire de Cristallochimie et de Chimie Structurale (UA 424), Institut LeBel, Université Louis Pasteur, 4 Rue Blaise Pascal, F-67070 Strasbourg Cedex, France, Department of Environmental Sciences and Engineering and Department of Chemistry, The University of North Carolina, Chapel Hill, North Carolina 27599, and Laboratoire de Chimie et Biochimie Pharmacologiques (UA 400), Université René Descartes, 45 Rue des St.-Pères, 75270 Paris Cedex 06, France

β-Halogenated-Pyrrole Porphyrins. Molecular Structures of 2,3,7,8,12,13,17,18-Octabromo-5,10,15,20-tetramesitylporphyrin, Nickel(II) 2,3,7,8,12,13,17,18-Octabromo-5,10,15,20-tetramesitylporphyrin, and Nickel(II) 2,3,7,8,12,13,17,18-Octabromo-5,10,15,20-tetrakis(pentafluorophenyl)porphyrin

D. Mandon,[1a] P. Ochsenbein,[1a] J. Fischer,[1a] R. Weiss,*[,1a] K. Jayaraj,[1b] R. N. Austin,[1b] A. Gold,*[,1b] P. S. White,[1c] O. Brigaud,[1d] P. Battioni,[1d] and D. Mansuy*[,1d]

Received October 4, 1991

The X-ray structures of the β-substituted-pyrrole tetraarylporphyrin 2,3,7,8,12,13,17,18-octabromo-5,10,15,20-tetramesitylporphyrin (H_2TMOBP), its nickel(II) complex (NiTMOBP), and the nickel(II) derivative of 2,3,7,8,12,13,17,18-octabromo-5,10,15,20-tetrakis(pentafluorophenyl)porphyrin (NiTPFPOBP·$^1/_2CH_2Cl_2$) are reported. The synthesis of the free base H_2TPFPOBP is also described. All these molecules are nonplanar, displaying saddle-shaped conformations. The saddle distortions minimize the intramolecular steric interactions between the bromine substituents and the ortho (ortho') carbon atoms or ortho (ortho') substituents of the phenyl rings, and consequently, the corresponding contact distances have similar values in all compounds. Because of the distortion of the porphyrin cores, the cavity defined by the ortho (ortho') substituents gives slightly less steric protection than in the nonbrominated nearly planar ortho- and ortho'-substituted tetraarylporphyrin complexes. Crystallographic data: $C_{56}H_{46}N_4Br_8$ (H_2TMOBP), tetragonal, space group $P\bar{4}2_1c$, $a = b = 15.085$ (4) Å, $c = 14.056$ (4) Å, $V = 3198.8$ Å^3, $Z = 2$, $R_F = 0.054$, $R_{wF} = 0.069$ based on 638 reflections with $I_o > 3\sigma(I_o)$, $T = 298$ K; $NiC_{56}H_{44}N_4Br_{8.18}$ (NiTMOBP), tetragonal, space group $P\bar{4}2_1c$, $a = b = 15.024$ (3) Å, $c = 14.068$ (6) Å, $V = 3175.2$ Å^3, $Z = 2$, $R_F = 0.049$, $R_{wF} = 0.057$ based on 877 reflections with $I_o > 2.5\sigma(I_o)$, $T = 298$ K; $NiC_{44}N_4F_{20}Br_8$·$^1/_2CH_2Cl_2$ (NiTPFPOBP·$^1/_2CH_2Cl_2$), monoclinic, space group $C2/c$, $a = 18.105$ (3) Å, $b = 22.141$ (5) Å, $c = 24.301$ (5) Å, $\beta = 93.32$ (2)°, $V = 9725.5$ Å^3, $Z = 8$, $R_F = 0.047$, $R_{wF} = 0.064$ based on 2896 reflections with $I_o > 3\sigma(I_o)$, $T = 298$ K.

Introduction

In the continuing development of (porphyrinato)iron complexes as catalysts for monooxygenation, halogenation of the pyrrole β-positions has been shown to confer on the catalyst properties of exceptional ruggedness and efficiency.[2,3] Promising β-halogenated porphyrin catalysts have been derived from the bromination of tetrakis(2,6-dichlorophenyl)porphyrin,[2a,b,g] tetramesitylporphyrin,[2c] and tetrakis(pentafluorophenyl)porphyrin.[2e] Indications are that substitution of the pyrrole β-positions with halogens causes S_4 distortion of the porphyrin to a saddle shape,[4] akin to that observed in the case of octaalkyl- and tetracycloalkenyl-substituted *meso*-tetraphenylporphyrins.[5] Such a distortion has been hypothesized to play an important role in altering the electronic structure and the chemistry of the oxoferryl π-cation-radical intermediates involved in catalytic oxidations.[2e,6,7]

Despite growing interest in halogenated porphyrins and their utility in catalysis, no crystal structure belonging to this novel class of porphyrins has been reported. As a part of a program underway in our laboratory to gain insight into the relationship between the chemistry and molecular structure of halogenated porphyrins and their metal complexes, we have attempted to crystallize several such compounds and wish to report here the molecular structures of tetramesityloctabromoporphyrin (H_2TMOBP), its nickel(II) complex (NiTMOBP), and the nickel derivative of tetrakis(pentafluorophenyl)octabromoporphyrin (NiTPFOBP).

Experimental Section

All syntheses were performed under dry argon, using distilled and degassed solvents. Pyrrole and mesitaldehyde were distilled before use; zinc acetate was heated overnight under vacuum; pentafluorobenzaldehyde, BF_3·Et_2O, chloranil, and 2,4,6-collidine were used as received. *N*-Bromosuccinimide (NBS) was purified by a published procedure[8] to remove traces of bromine. Porphyrin free bases and metal complexes were characterized by UV-vis and NMR spectroscopy and mass spectrometry. ^{1}H NMR spectra were recorded on a Bruker SY 200 spectrometer at 200 MHz or a Varian XL 400 spectrometer at 400 MHz, and ^{19}F NMR spectra, on a Bruker AC 200 instrument at 200 MHz. Chemical shifts of ^{1}H resonances are given in ppm relative to TMS, and ^{19}F shifts, in ppm relative to $CFCl_3$. Electronic spectra were obtained on a Cary 219 spectrometer.

Preparation and Characterization of H_2TMOBP and Ni^{II}TMOBP. H_2TMP and its octabrominated derivative H_2TMOBP were synthesized according to published procedures.[2c,9] H_2TMOBP obtained after an initial chromatography over alumina was contaminated with meta-brominated-phenyl impurities, estimated at 4-8% from integration of the side signals in the ^{1}H NMR spectra and residual electron density within bonding distance of the phenyl meta positions in the X-ray structure obtained with "first crop" single crystals.[10] Purification of this mixture was achieved by four successive crystallizations in methylene chloride/*n*-hexane. Single crystals suitable for X-ray studies were obtained by slow diffusion of hexane into a chloroform solution of purified H_2TMOBP.

ZnTMOBP. UV-vis (methylene chloride): λ_m 462, 592, 637 nm. ^{1}H NMR (200 MHz, methylene-d_2 chloride): δ 7.22 (8 H, s, *m*-H of phe-

(1) (a) Université Louis Pasteur. (b) Department of Environmental Sciences and Engineering, The University of North Carolina. (c) Department of Chemistry, The University of North Carolina. (d) Université René Descartes.
(2) (a) Traylor, T. G.; Tsuchiya, S. *Inorg. Chem.* **1987**, *26*, 1338-1339. (b) Tsuchiya, S.; Seno, M. *Chem. Lett.* **1989**, 263-266. (c) Hoffman, P.; Labat, G.; Robert, A.; Meunier, B. *Tetrahedron Lett.* **1990**, *31*, 1991-1994. (d) Wijesekera, T.; Matsumoto, A.; Dolphin, D.; Lexa, D. *Angew. Chem.* **1990**, *102*, 1073-1074. (e) Bartoli, J. F.; Brigaud, O.; Battioni, P.; Mansuy, D. *J. Chem. Soc., Chem. Commun.* **1991**, 440. (f) Gonsalves, A. M.; Jonstone, R. A. W.; Pereira, M. M.; Shaw, J.; Sobral, J. F. *Tetrahedron Lett.* **1991**, *32*, 1355-1358. (g) Battioni, P.; Brigaud, O.; Desvaux, H.; Mansuy, D.; Traylor, T. G. *Tetrahedron Lett.* **1991**, *32*, 2893-2896.
(3) Dolphin, D. H.; Kekeno, T.; Kirk, T. K.; Marone, T. E.; Farrell, R. L.; Wijesekera, T. P. Patent PCT Int. Appl. WO88/07, 1987.
(4) Bhyrappa, P.; Krishnan, V. *Inorg. Chem.* **1991**, *30*, 239.
(5) (a) Barkigia, K. M.; Chantraupong, L.; Smith, K. M.; Fajer, J. *J. Am. Chem. Soc.* **1988**, *110*, 7566-7567. (b) Medforth, C. J.; Berber, D.; Smith, K. M.; Shelnutt, J. A. *Tetrahedron Lett.* **1990**, *31*, 3719-3722. (c) Barkigia, K. M.; Barber, M. D.; Fajer, J.; Medforth, G. J.; Renner, M. W.; Smith, K. M. *J. Am. Chem. Soc.* **1990**, *112*, 8851-8857. (d) Shelnutt, J. A.; Medforth, C. J.; Berber, M. D.; Barkigia, K. M.; Smith, K. M. *J. Am. Chem. Soc.* **1991**, *113*, 4077-4087.
(6) (a) Boso, B.; Lang, G.; McMurry, T. J.; Groves, J. T. *J. Chem. Phys.* **1983**, *79*, 1122-1126. (b) Groves, J. T.; Quinn, R.; McMurry, T. J.; Nakamura, M.; Lang, G.; Boso, B. *J. Am. Chem. Soc.* **1985**, *107*, 354-360. (c) Groves, J. T.; Watanabe, Y. *Ibid.* **1988**, *110*, 8443-8452.
(7) Hashimoto, S.; Mizutani, Y.; Tatsuno, Y.; Kitagawa, T. *J. Am. Chem. Soc.* **1991**, *113*, 6542-6549.
(8) Perrin, D. D.; Armarego, W. L. F. *Purification of Laboratory Chemicals*, 3rd ed.; Pergamon Press: New York, 1988; p 105.
(9) Kihn-Botulinsky, M.; Meunier, B. *Inorg. Chem.* **1988**, *27*, 209-210.
(10) These crystals were obtained by slow diffusion of hexane into chloroform solutions of freshly prepared H_2TMOBP before purification by further crystallizations.

0020-1669/92/1331-2044$03.00/0

Table I. X-ray Experimental Parameters

	H_2TMOBP	NiTMOBP	NiTPFPOBP
formula	$C_{56}H_{46}N_4Br_8$	$C_{56}H_{44}N_4NiBr_{8.18}$	$C_{44}N_4F_{20}NiBr_8$ $1/2CH_2Cl_2$
mol wt	1414.29	1485.31	1704.93
color	black	purple	dark green
cryst system	tetragonal	tetragonal	monoclinic
a, Å	15.085 (4)	15.024 (3)	18.105 (3)
b, Å			22.141 (5)
c, Å	14.056 (4)	14.068 (6)	24.301 (5)
β, deg			93.32 (2)
V, Å^3	3198.8	3175.2	9725.5
Z	2	2	8
D_{calc}, g cm^{-1}	1.468	1.553	2.329
space group	$P\bar{4}2_1c$ (No. 114)	$P\bar{4}2_1c$ (No. 114)	$C2/c$ (No. 15)
radiation		Mo Kα (graphite monochromated)	
wavelength, Å		0.710 73	
μ, cm^{-1}	50.0	54.4	70.8
cryst size, mm	0.30/0.30/0.10	0.20/0.20/0.20	0.30/0.20/0.12
temp, °C		20	
diffractometer	Enraf-Nonius CAD4-F	Rigaku AFC6S	Enraf-Nonius CAD4-F
mode		AFC6S $\theta/2\theta$ scan	
scan speed, deg^{-1}	variable	multiple scans	variable
scan width, deg	1.00 + 0.343 tan θ	1.00 + 0.35 tan θ	1.00 + 0.343 tan θ
θ limits, deg	2/24	3/25	2/25
octants	$+h,+k,+l$	$+h,+k,+l$	$\pm h,+k,+l$
no. of data collcd	5438	3067	8969
no. of unique data	638 ($I > 3\sigma(I)$)	877 ($I > 2.5\sigma(I)$)	2896 ($I > 3\sigma(I)$)
$R_{int}(F)$	0.032	0.064	0.032
abs, min/max	0.79/0.99	0.35/0.45	0.62/0.99
$R(F)$	0.054	0.049	0.047
$R_w(F)$	0.069	0.057	0.064
p	0.08	0.05	0.08
GOF	1.26	1.82	1.46

nyl), 2.56 (12 H, s, *p*-methyl), 1.88 (24 H, s, *o*-methyl).

H_2TMOBP. UV–vis (methylene chloride): λ_m (ϵ, mM^{-1} cm^{-1}) 465 (198), 559 (8.8), 605 (7.0) nm. ^{1}H NMR (200 MHz, methylene-d_2 chloride): δ 7.22 (8 H, s, *m*-H of phenyl), 2.55 (12 H, s, *p*-methyl), 1.99 (24 H, s, *o*-methyl), −1.29 (2 H, s, NH). The FAB mass spectrum (magic bullet matrix) showed a cluster centered at m/z 1415 (MH$^+$), isotope pattern in accord with Br_8 substitution.

H_2TMOBP was metalated with nickel by refluxing with nickel(II) acetate, $Ni(OAc)_2{\cdot}4H_2O$, in DMF for 15 min. After removal of the solvent under reduced pressure, the solid residue was purified by column chromatography over silica with chloroform eluant. Crystals suitable for X-ray studies were obtained by slow diffusion of pentane into a methylene chloride solution of the nickel complex.

NiTMOBP. UV–vis (chloroform): λ_m (ϵ, mM^{-1} cm^{-1}) 449 (245), 561 (18.0), 593 (6.5) nm. ^{1}H NMR (400 MHz, methylene-d_2 chloride): δ 7.13 (8 H, *m*-H of phenyl), 2.50 (12 H, *p*-methyl), 1.83 (24 H, *o*-methyl). The FAB mass spectrum (magic bullet matrix) showed a cluster having a center of gravity at m/z = 1470 (MH$^+$), isotope pattern in accord with the presence of Ni and Br_8 substitution.

Preparation and Characterization of NiTPFPOBP. NiTBFPOBP was prepared in three steps from ZnTPFPP.

ZnTPFPP was brominated by a modified version of a procedure reported for polybromination of porphyrins.[2a,11] Trifluoroacetic acid (1.5 mL, 20 mmol) was slowly added during 48 h to a refluxing solution of ZnTPFPP (1.06 g, 1 mmol) and *N*-bromosuccinimide (7.2 g, 40 mmol) in a $CHCl_3/CHCl_2CHCl_2$ mixture (1:1, 200 mL). After cooling, $Zn(OAc)_2$ (0.22 g, 1 mmol) was added in order to completely metalate any free base formed during the reaction. After neutralization by NaOH and evaporation of the solvents, ZnTPFPOBP was purified by column chromatography (neutral alumina, CH_2Cl_2 as eluant, yield 70%).

ZnTPFOBP. UV–vis (CH_2Cl_2): λ_m (ϵ, mM^{-1} cm^{-1}) 460 (211), 590 (17.8). ^{19}F NMR (200 MHz, chloroform-d_1): δ −137.5 (8 F, *o*), −150.5 (4 F, *p*), −162.2 (8 F, *m*). The mass spectrum (chemical ionization, NH_3) showed a cluster with center of gravity at m/z = 1670 (MH$^+$) (superimposable on the theoretical cluster).

ZnTPFPOBP (0.6 g, 0.35 mmol) was demetalated by stirring with trifluoroacetic acid (2 mL) in methylene chloride (2 mL) over 24 h at room temperature. The mixture was poured into ice, carefully neutralized, extracted with CH_2Cl_2, and dried over Na_2SO_4. After evaporation of the solvent, H_2TPFPOBP was obtained in a 92% yield by column chromatography over neutral alumina, with 1:1 methylene chloride/pentane as eluant.

H_2TPFPOBP. UV–vis (CH_2Cl_2): λ_m (ϵ, mM^{-1} cm^{-1}) 453 (186), 553 (18.8), 633 (6.3) nm. ^{1}H NMR (400 MHz, chloroform-d_1): δ −1.67 (2 H, s, NH). ^{19}F NMR (200 MHz, chloroform-d_1): δ = −137.6 (8 F, *o*), −149.0 (4 F, *p*) and −161.4 (8 F, *m*).

H_2TPFPOBP (0.1 g, 0.06 mol) dissolved in 5 mL of CH_2Cl_2 was metalated by refluxing with $Ni(OAc)_2{\cdot}4H_2O$ (0.1 g, 0.4 mmol) in 5 mL of methanol. The reaction was taken to complete dryness, the solid residue was redissolved in CH_2Cl_2, the mixture was washed with water, and the organic layer was dried over Na_2SO_4 and evaporated. Column chromatography over neutral alumina with CH_2Cl_2 as eluant gave the nickel complex NiTPFPOBP in 92% yield. Single crystals suitable for X-ray studies were obtained by slow evaporation in air of 1:1 dichloromethane/decane solutions of the nickel complex of H_2TPFOBP.

NiTPFPOBP. UV–vis (CH_2Cl_2): λ_m (ϵ, mM^{-1} cm^{-1}) 436 (208), 560 (15.8), 600 (22.6) nm. ^{19}F NMR (200 MHz, chloroform-d_1): δ −137.2 (8 F, *o*), −149.5 (4 F, *p*), −161.5 (8 F, *m*). The mass spectrum (chemical ionization, NH_3) showed a cluster with center of gravity at m/z = 1664 (MH$^+$), isotope pattern consistent with the presence of Ni and Br_8 substitution.

X-ray Experimental Section

X-ray data on H_2TMOBP and NiTPFPOBP were collected on an Enraf-Nonius CAD4-F diffractometer, and data on NiTMOBP, on a Rigaku AFC6S instrument. Single crystals of H_2TMOBP and NiTPFPOBP were cut out from clusters; those of NiTMOBP were recovered without additional preparation from the mother liquor after crystallization was complete. A systematic search in reciprocal space showed that the crystals of H_2TMOBP and NiTMOBP belonged to the tetragonal system and those of NiTPFPOBP to the monoclinic system. Although H_2TMOBP and NiTPFPOBP readily yielded crystals of satisfactory appearance under the microscope, analysis of reflections from a large number of crystals from several crystallization experiments showed diffraction peaks which were broad and somewhat asymmetric. Crystal data for all three compounds are given in Table I.

Quantitative data were obtained at room temperature. All experimental parameters used are given in Table I. Three standard reflections measured every 1 h during data collection on the Nonius diffractometer and every 150 reflections on the Rigaku instrument showed no significant trend. The data sets obtained on the CAD4-F instrument were transferred to a VAX computer, and for all subsequent calculations the Enraf-Nonius SDP/VAX package[12a] was used. Data from the Rigaku

(11) Callot, H. J. *Bull. Soc. Chim. Fr.* **1974**, 1492–1496.

Table II. Positional and Thermal Parameters and Their Esd's

atom	x	y	z	B,[a] Å^2
Br1	0.2685 (1)	0.2187 (1)	0.3523 (2)	4.36 (5)
Br2	0.4650 (2)	0.1194 (1)	0.4042 (2)	4.50 (5)
N	0.445 (1)	0.377 (1)	0.490 (2)	3.3 (4)
C1	0.359 (1)	0.361 (1)	0.464 (2)	2.4 (4)
C2	0.357 (1)	0.274 (1)	0.423 (2)	2.2 (4)
C3	0.437 (1)	0.235 (1)	0.441 (2)	3.2 (5)
C4	0.497 (1)	0.299 (1)	0.486 (1)	2.1 (4)
C5	0.290 (1)	0.420 (1)	0.478 (2)	2.5 (5)
C6	0.196 (1)	0.388 (1)	0.458 (2)	3.0 (5)
C7	0.160 (1)	0.328 (1)	0.521 (1)	2.8 (5)
C8	0.064 (2)	0.299 (1)	0.498 (2)	6.0 (7)
C9	0.026 (1)	0.331 (2)	0.411 (2)	5.2 (6)
C10	0.069 (1)	0.389 (1)	0.356 (3)	6.7 (9)
C11	0.154 (1)	0.417 (1)	0.380 (2)	3.9 (6)
C12	0.205 (2)	0.295 (2)	0.612 (2)	4.8 (6)
C13	−0.064 (2)	0.292 (2)	0.389 (3)	8 (1)
C14	0.197 (2)	0.480 (2)	0.303 (3)	6.2 (7)

[a] B values for anisotropically refined atoms are given in the form of the isotropic equivalent displacement parameter defined as $(4/3)[a^2\beta(1,1) + b^2\beta(2,2) + c^2\beta(3,3) + ab(\cos\gamma)\beta(1,2) + ac(\cos\beta)\beta(1,3) + bc(\cos\alpha)\beta(2,3)]$.

Table III. Positional and Thermal Parameters and Their Esd's

	x	y	z	B_{iso},[a] Å^2
Ni	1/2	1/2	0	2.40 (13)
Br1	0.77843 (14)	0.27405 (13)	−0.15357 (15)	4.41 (9)
Br2	0.88017 (11)	0.46736 (12)	−0.08955 (16)	4.51 (10)
N	0.6159 (8)	0.4484 (7)	−0.0138 (9)	2.1 (5)
C1	0.6325 (12)	0.3651 (11)	−0.0479 (11)	2.9 (8)
C2	0.7237 (10)	0.3638 (11)	−0.0853 (13)	3.3 (8)
C3	0.7621 (10)	0.4410 (10)	−0.0566 (11)	2.7 (7)
C4	0.6964 (9)	0.4962 (11)	−0.0154 (10)	2.1 (7)
C5	0.5778 (10)	0.2924 (10)	−0.0260 (11)	2.3 (7)
C6	0.6102 (6)	0.2001 (5)	−0.0469 (6)	3.3 (8)
C7	0.5805 (7)	0.1553 (6)	−0.1277 (7)	4.4 (10)
C8	0.6112 (8)	0.0696 (6)	−0.1472 (7)	5.9 (12)
C9	0.6715 (7)	0.0287 (5)	−0.0858 (8)	5.1 (11)
C10	0.7012 (6)	0.0735 (5)	−0.0049 (7)	5.0 (11)
C11	0.6705 (6)	0.1592 (5)	0.0145 (6)	3.3 (8)
C12	0.5139 (10)	0.2005 (8)	−0.1955 (9)	6.1 (11)
C13	0.7054 (11)	−0.0660 (6)	−0.1073 (12)	8.4 (15)
C14	0.7033 (9)	0.2086 (8)	0.1038 (8)	4.3 (9)
Br3	0.786 (3)	0.016 (3)	0.053 (3)	3.9 (9)

[a] B values for anisotropically refined atoms are given in the form of the isotropic equivalent displacement parameter defined as $(4/3)[a^2\beta(1,1) + b^2\beta(2,2) + c^2\beta(3,3) + ab(\cos\gamma)\beta(1,2) + ac(\cos\beta)\beta(1,3) + bc(\cos\alpha)\beta(2,3)]$.

diffractometer were processed on a DEC station computer using the NRCVAX software package. All the raw data sets were corrected for Lorentz and polarization factors, and the intensities of equivalent reflections were averaged. All the intensity profiles were recorded for NiTPFPOBP, and in order to minimize possible effects due to partial peak overlap, the net intensity of each reflection was determined by profile analysis using the Lehman–Larsen method.[12b] Semiempirical absorption corrections based on ψ-scans were applied to the data. The structures of H_2TMOBP and NiTPFPPOBP were solved using SIR[13] to locate the heavy atoms. After refinement of these atoms, a difference-Fourier map of H_2TMOBP revealed a maxima of residual electronic density close to the positions expected for hydrogen atoms; they were introduced in the structure factor calculations by their computed coordinates (C–H = 0.95 Å) and isotropic temperature factors such as B(H) = 1.3 B_{eqv}(C) Å^2 but not refined; the H–N hydrogens of H_2TMOBP and the solvate hydrogens of NiTPFPOBP were omitted. Full-matrix least-squares refinements on F proceeded under the conditions $\sigma^2(F^2) = \sigma^2_{counts} + (pI)^2$. Final difference maps revealed no significant maxima. The scattering factor coefficients and anomalous dispersion coefficients come respectively from ref 14a,b.

The structure of NiTMOBP was solved using the solver[15] direct methods routine to locate the nickel and bromine atom positions. The remaining atoms were located from subsequent difference-Fourier syntheses. Hydrogen atoms were included in the final refinement at computed positions with a C–H bond length of 0.95 Å. Because of the large number of parameters, the crystallographically independent phenyl ring was refined as a rigid body. Final cycles of least-squares refinements revealed a 4% porphyrin impurity having bromine at the meta position of the phenyl ring. The presence of a nonabrominated impurity was verified in the FAB mass spectrum of the crystals.

H_2TMOBP and NiTMOBP crystallize in space group $P\bar{4}2_1c$ with two porphyrins per unit cell. The macrocycles lie on a 4-fold inversion axis: therefore, the crystallographically required symmetry is S_4. Because of the two pyrrole NH groups, the symmetry of the free base cannot, in this orientation, exceed S_2 (C_{2h}) and is, therefore, 2-fold disordered around the 4-fold inversion axis. Tables II and III list the positional parameters for the independent non-hydrogen atoms of H_2TMOBP and NiTMOBP.

The crystals of NiTPFPOBP contain CH_2Cl_2 molecules of solvation in the ratio 1:2 CH_2Cl_2/NiTPFPOBP. The CH_2Cl_2 molecules lie on a 2-fold axis whereas the NiTPFPOBP molecules lie in general positions of space group $C2/c$. Table IV lists the positional parameters for all non-hydrogen atoms.

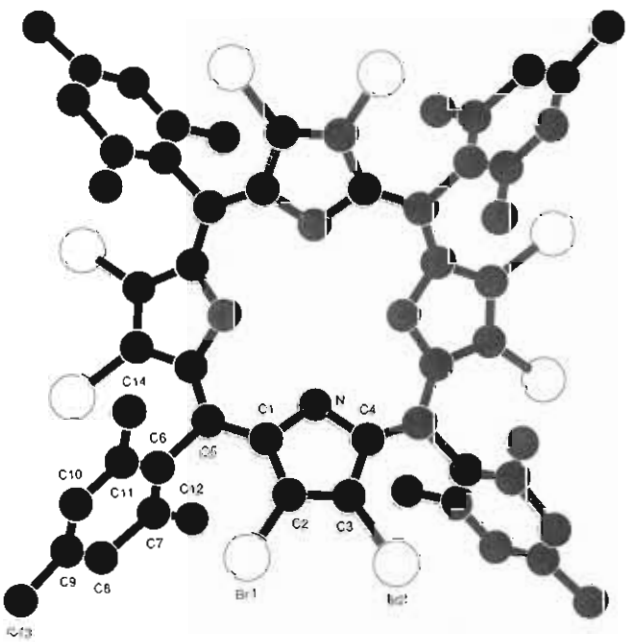

Figure 1. CAP[12c] plot of one molecule of H_2TMOBP, showing the numbering scheme used. Hydrogen atoms are omitted.

Results and Discussion

The molecular structures of H_2TMOBP and NiTPFPOBP are displayed in Figures 1 and 2 together with the labeling schemes used for the crystallographically independent atoms in the structures.

It has been shown recently that crowded porphyrin peripheries such as those present in the zinc complexes of the 2,3,7,8,12,13,17,18-octamethyl- and 2,3,7,8,12,13,17,18-octaethyltetraphenylporphyrins Zn(py)OMTPP and Zn(CH_3OH)OETPP lead to severe S_4 saddle distortions of the macrocycles.[5a–d] The same type of distortion occurs in the structures of the three brominated porphyrins determined in this study. These structures show that the pyrrole rings with the, approximately coplanar, bromine substituents are tilted alternatively up and down relative to the mean porphyrin plane defined by the 24-atom core, as well as being twisted relative to this mean plane which defines the horizontal. The meso phenyl rings show similar alternating vertical displacements, and their mean planes are rotated toward the

(12) (a) Frenz, B. A. The Enraf-Nonius CAD4-SDP. In *Computing in Crystallography*; Schenk, H., Olthof-Hazekamp, R., Van Koningveld, H, Bassi, G. C., Eds.; Delft University Press: Delft, The Netherlands, 1978; pp 64–71. (b) Lehman, M. S.; Larsen, F. K. *Acta Crystallogr., Sect. A: Cryst. Phys., Diffr., Theor. Gen. Crystallogr.* **1974**, *A30*, 580. (c) CAP is a molecular plotting program written by J. W. Lauher, Department of Chemistry, SUNY, Stony Brook, NY.
(13) Burla, M. C.; Cascarano, G.; Giacovazzo, C.; Nunzi, A.; Polidori, G. *Acta Crystallogr.* **1987**, *A43*, 370–374.
(14) Cromer, D. T.; Waber, J. T. *International Tables for X-ray Crystallography*; The Kynoch Press: Birmingham, England, 1974; Vol. IV, (a) Table 2.2b, (b) Table 2.3.1.
(15) Gabe, E. J.; LePage, Y.; Charland, J.-P.; Lee, F. L.; White, P. S. *J. Appl. Crystallogr.* **1989**, 384–387.

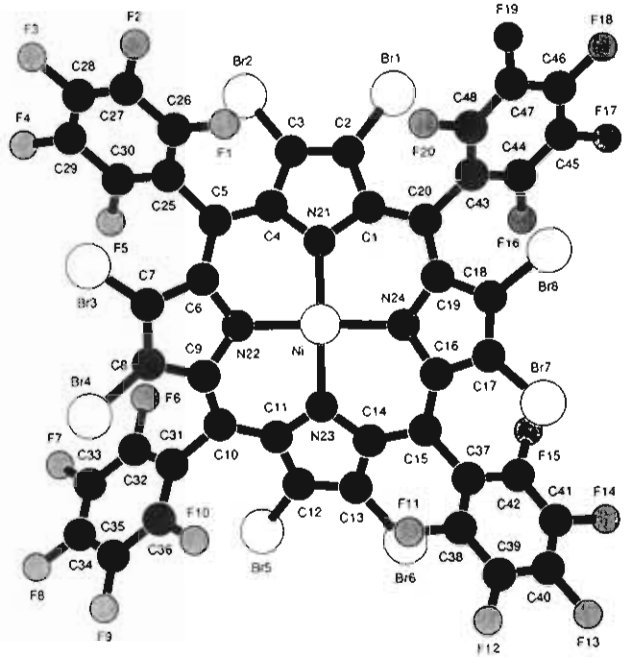

Figure 2. CAP[12c] plot of one molecule of NiTPFPOBP, showing the numbering scheme used.

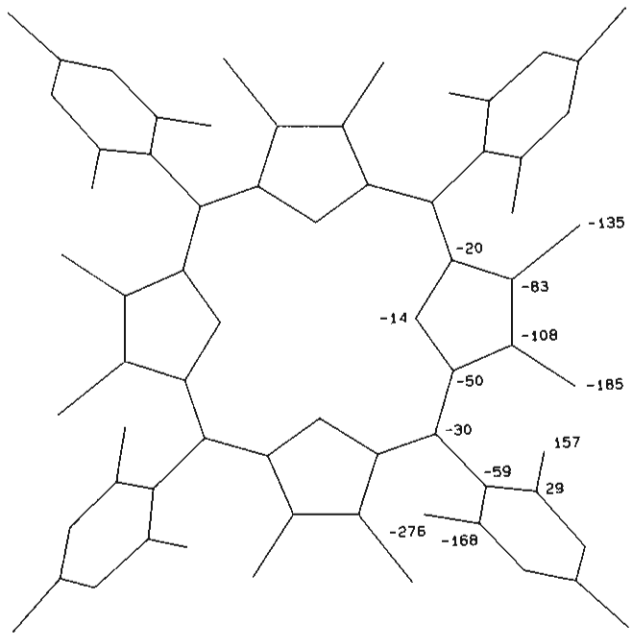

Figure 3. PLUTO plot of one molecule of H_2TMOBP in the same orientation as for Figure 1. Numbers in parentheses indicate the deviations of all atoms (in 0.01 Å units) with respect to the 24-core-atom mean plane.

24-atom core mean planes of the porphyrins in order to minimize the intramolecular steric interactions between the bromines and the ortho- and ortho′-carbon atoms (*o*-C and *o*′-C) and substituents of the phenyl rings. The perpendicular displacements (in 0.01 Å) of the porphyrin core atoms and bromine substituents of H_2TMOBP, NiTMOBP, and NiTPFPOBP relative to their 24-atom-core mean planes are indicated in Figures 3–5, and Figure 6 displays an edge-on view of the 24-atom core and bromine substituents of H_2TMOBP to illustrate the core shape. Table V gives selected bond lengths and angles, and intermolecular contact distances for all three molecules are listed in the supplementary material.

The perpendicular displacements of the bromine and pyrrole β-carbon atoms from the mean porphyrin plane of H_2TMOBP are 1.85 (Br1), 1.35 (Br2), 1.08 (C2), and 0.83 Å (C3). For NiTMOBP, the corresponding displacements are: 2.16 (Br1), 1.26

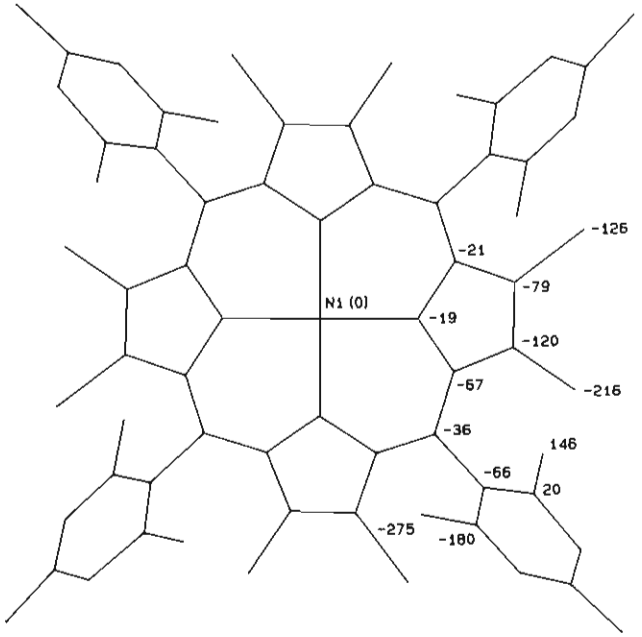

Figure 4. PLUTO plot of one molecule of NiTMOBP in the same orientation as for Figure 3. The numbering scheme used for the atoms in NiTMOBP is identical to that adopted for H_2TMOBP. Numbers in parentheses indicate the deviations of all atoms (in 0.01 Å units) with respect to the 24-core-atom mean plane.

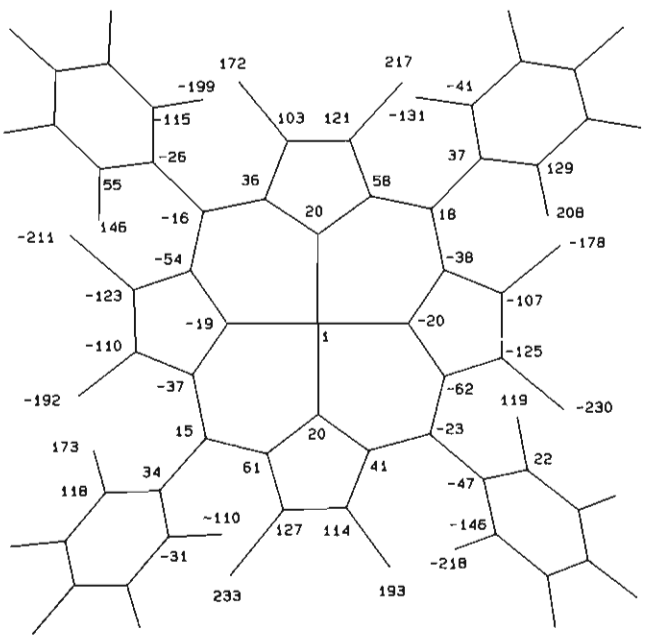

Figure 5. PLUTO plot of one molecule of NiTPFPOBP in the same orientation as for Figure 3. Numbers in parentheses indicate the deviations of all atoms (in 0.01 Å units) with respect to the 24-core-atom mean plane.

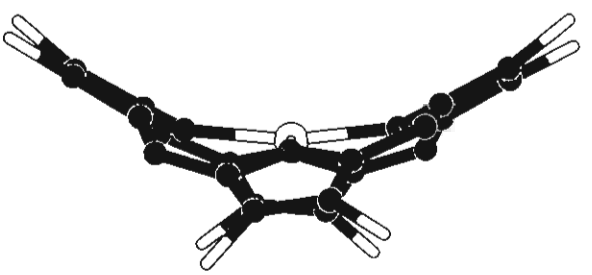

Figure 6. "Edge-on" view CAP[12c] plot of the skeleton of NiTPFOBP. (The meso substituents have been removed for clarity.)

(Br2), 1.20 (C2), and 0.80 (C3) Å. For NiTPFPOBP, the average absolute perpendicular shifts are 2.23 (Br1,3,5,7), 1.84 (Br2,4,6,8),

Table IV. Positional and Thermal Parameters and Their Esd's

atom	x	y	z	B,[a] Å²	atom	x	y	z	B,[a] Å²
Ni	0.6787 (1)	0.09913 (8)	0.02522 (8)	1.52 (4)	F2	0.3154 (7)	0.2958 (6)	0.0192 (6)	8.0 (4)
Br1	0.7017 (1)	0.35503 (8)	0.06979 (9)	4.41 (5)	F3	0.2690 (6)	0.2970 (6)	−0.0909 (7)	11.4 (4)
Br2	0.5656 (1)	0.33540 (9)	−0.03291 (9)	4.31 (5)	F4	0.3529 (7)	0.2465 (6)	−0.1653 (5)	7.4 (3)
Br3	0.3757 (1)	0.0920 (1)	−0.0594 (1)	4.90 (5)	F5	0.4823 (6)	0.1925 (5)	−0.1340 (4)	4.9 (3)
Br4	0.4599 (1)	−0.0369 (1)	−0.10320 (9)	4.58 (5)	C31	0.6320 (9)	−0.0361 (7)	−0.1264 (7)	2.6 (4)
Br5	0.8041 (1)	−0.0618 (1)	−0.12968 (8)	5.17 (5)	C32	0.624 (1)	−0.0109 (8)	−0.1792 (7)	3.7 (5)
Br6	0.9188 (1)	−0.0657 (1)	−0.01258 (9)	5.17 (5)	C33	0.609 (1)	−0.044 (1)	−0.2270 (7)	5.3 (6)
Br7	0.8333 (1)	0.0128 (1)	0.22437 (8)	4.78 (5)	C34	0.602 (1)	−0.1019 (9)	−0.2249 (8)	4.5 (6)
Br8	0.7818 (1)	0.15816 (9)	0.24928 (8)	4.27 (5)	C35	0.611 (1)	−0.1318 (9)	−0.1773 (8)	4.4 (6)
C1	0.6829 (8)	0.2200 (6)	0.0699 (7)	2.6 (4)	C36	0.624 (1)	−0.0979 (8)	−0.1276 (7)	3.7 (5)
C2	0.6610 (9)	0.2813 (7)	0.0486 (6)	2.6 (4)	F6	0.6320 (9)	0.0494 (5)	−0.1808 (5)	7.9 (4)
C3	0.6069 (9)	0.2742 (7)	0.0113 (6)	2.0 (4)	F7	0.604 (1)	−0.0142 (7)	−0.2738 (5)	11.1 (5)
C4	0.5920 (9)	0.2093 (7)	0.0055 (6)	2.2 (4)	F8	0.5862 (8)	−0.1333 (6)	−0.2707 (5)	10.7 (4)
C5	0.5324 (9)	0.1816 (7)	−0.0230 (6)	2.3 (4)	F9	0.6039 (9)	−0.1917 (5)	−0.1736 (6)	8.8 (4)
C6	0.5351 (8)	0.1193 (7)	−0.0318 (6)	1.6 (3)	F10	0.6321 (7)	−0.1280 (4)	−0.0784 (5)	6.0 (3)
C7	0.4782 (9)	0.0801 (8)	−0.0572 (6)	3.0 (4)	C37	0.8675 (8)	−0.0339 (7)	0.1059 (6)	2.0 (3)
C8	0.5116 (9)	0.0287 (7)	−0.0731 (6)	1.9 (4)	C38	0.8517 (9)	−0.0934 (8)	0.1146 (7)	2.8 (4)
C9	0.5884 (9)	0.0344 (7)	−0.0578 (5)	1.6 (3)	C39	0.903 (1)	−0.1337 (7)	0.1358 (8)	5.1 (5)
C10	0.6467 (9)	0.0012 (6)	−0.0763 (5)	1.7 (3)	C40	0.969 (1)	−0.112 (1)	0.1508 (9)	5.2 (6)
C11	0.7151 (8)	0.0016 (6)	−0.0496 (6)	1.6 (3)	C41	0.986 (1)	−0.054 (1)	0.1418 (9)	6.6 (7)
C12	0.7786 (9)	−0.0303 (6)	−0.0619 (6)	2.1 (4)	C42	0.937 (1)	−0.0143 (8)	0.1208 (7)	5.4 (4)
C13	0.8241 (8)	−0.0307 (7)	−0.0164 (6)	1.8 (3)	F11	0.7827 (6)	−0.1132 (4)	0.1010 (4)	4.6 (3)
C14	0.7898 (8)	0.0031 (7)	0.0232 (6)	1.9 (3)	F12	0.8820 (8)	−0.1899 (5)	0.1429 (5)	7.5 (4)
C15	0.8137 (9)	0.0092 (7)	0.0808 (6)	1.9 (3)	F13	1.0202 (8)	−0.1530 (6)	0.1725 (7)	14.4 (5)
C16	0.7829 (8)	0.0550 (7)	0.1123 (7)	2.3 (4)	F14	1.0602 (7)	−0.0353 (7)	0.1540 (7)	10.0 (5)
C17	0.7979 (8)	0.0660 (7)	0.1704 (6)	2.0 (3)	F15	0.9567 (6)	0.0414 (5)	0.1134 (5)	5.8 (3)
C18	0.7777 (9)	0.1221 (7)	0.1794 (6)	2.0 (4)	C43	0.7468 (9)	0.2550 (6)	0.1582 (6)	3.0 (4)
C19	0.7453 (8)	0.1471 (7)	0.1282 (6)	1.6 (3)	C44	0.820 (1)	0.2734 (7)	0.1683 (8)	3.5 (4)
C20	0.7257 (8)	0.2068 (7)	0.1177 (6)	2.1 (4)	C45	0.8366 (9)	0.3144 (8)	0.2074 (8)	3.6 (4)
N21	0.6448 (6)	0.1782 (5)	0.0372 (5)	1.6 (3)	C46	0.785 (1)	0.3417 (8)	0.2377 (7)	4.0 (5)
N22	0.6008 (6)	0.0866 (5)	−0.0291 (5)	1.8 (3)	C47	0.715 (1)	0.3264 (8)	0.2256 (7)	5.4 (5)
N23	0.7259 (7)	0.0274 (5)	0.0019 (5)	1.6 (3)	C48	0.6964 (9)	0.2829 (7)	0.1897 (7)	2.6 (4)
N24	0.7444 (7)	0.1029 (5)	0.0893 (4)	1.6 (3)	F16	0.8716 (5)	0.2488 (5)	0.1378 (5)	4.7 (3)
C25	0.4648 (8)	0.2151 (7)	−0.0411 (6)	2.1 (4)	F17	0.9071 (6)	0.3300 (5)	0.2171 (5)	5.8 (3)
C26	0.422 (1)	0.2424 (8)	−0.0025 (9)	4.1 (5)	F18	0.8052 (8)	0.3830 (5)	0.2752 (5)	7.2 (4)
C27	0.355 (1)	0.2708 (9)	−0.021 (1)	5.3 (5)	F19	0.6620 (7)	0.3525 (5)	0.2555 (5)	7.1 (3)
C28	0.334 (1)	0.2706 (9)	−0.0723 (9)	5.0 (5)	F20	0.6239 (5)	0.2658 (5)	0.1821 (4)	4.6 (3)
C29	0.373 (1)	0.2467 (8)	−0.1132 (8)	5.0 (5)	C49	0.000	0.192 (2)	0.250	8 (1)
C30	0.444 (1)	0.2183 (8)	−0.0963 (7)	3.8 (4)	Cl	0.0032 (5)	0.1471 (4)	0.1918 (4)	12.1 (3)
F1	0.4446 (6)	0.2423 (5)	0.0498 (4)	4.9 (3)					

[a] *B* values for anisotropically refined atoms are given in the form of the isotropic equivalent displacement parameter defined as $(4/3)[a^2\beta(1,1) + b^2\beta(2,2) + c^2\beta(3,3) + ab(\cos\gamma)\beta(1,2) + ac(\cos\beta)\beta(1,3) + bc(\cos\alpha)\beta(2,3)]$.

1.24 (C2,7,12,17), and 1.08 Å (C3,8,13,18). A comparison of these displacements shows that the distortion of the free base is slightly less severe than that occurring in the nickel complexes. The reason for this difference is, probably, the presence of a small nickel(II) cation[16] in the macrocyclic cavities causing core contraction. For the free-base H_2TMOBP, the radius of the central cavity, N_p--C_t, is 2.04 (2) Å (C_t = center of the 24-atom core) and is distinctly larger than the value of the Ni–N_p bond length of 1.916 (12) Å in NiTMOBP and the average Ni–N_p bond distance of 1.898 (10) Å in NiTPFPOBP. The saddle distortion does not, however, cause the Ni–N_p bond distances in the brominated complexes to differ significantly from the average Ni–N_p bond distance occurring in the S_4-ruffled NiOEP complex (1.929 (3) Å)[17] and results in only a slightly smaller average Ni–N_p bond length than in the nearly planar NiOEP derivative (1.958 (2) Å)[18] (OEP = octaethylporphyrin dianion). In all three brominated porphyrins, minimization of the intramolecular steric interactions by the saddle distortion[19] is evident by the similarity of the contact distances between the bromine atoms and adjacent *o*- and *o'*-C atoms of the phenyl group. However, these nonbonding contact distances are not unreasonably short. In H_2TMOBP, the relevant nonbonding separations are Br1--(*o*-C) = 3.32, Br1--(*o'*-C) = 3.48, Br2--(*o*-C) = 3.35, and Br2--(*o'*-C) = 3.55 Å; in NiTMOBP, Br1--(*o*-C) = 3.32, Br1--(*o'*-C) = 3.48, Br2--(*o*-C) = 3.35, and Br2--(*o'*-C) = 3.55 Å; in NiTPFPOBP, Br(1,3,5,7)--(*o*-C) = 3.33, Br(2,4,6,8)--(*o*-C) = 3.38, Br(1,3,5,7)--(*o'*-C) = 3.63, and Br(2,4,6,8)--(*o'*-C) = 3.55 Å. For the tetramesityl derivatives, the nonbonding contact distances between Br1 and Br2 and the *o*- and *o'*-Me groups on adjacent mesityl substituents are for

Table V. Selected Bond Lengths (Å), Bond Angles (deg), and Averages with Their Estimated Standard Deviations[a]

	H_2TMOBP	NiTMPBP	NiTPFPOBP
C_t–N_p	2.04 (2)		
Ni–N_p		1.916 (12)	
Ni–N21			1.884 (10)
Ni–N22			1.896 (10)
Ni–N23			1.906 (10)
Ni–N24			1.898 (10)
⟨N_p–Ni–N_p⟩cis		90.6 (5)	90.6 (6)
⟨N_p–Ni–N_p⟩trans		168.4 (5)	168.0 (6)
N–C_α	1.40 (3)	1.39 (2)	1.37 (1)
C_α–C_β	1.44 (3)	1.44 (2)	1.44 (3)
C_β–C_β	1.37 (3)	1.36 (2)	1.32 (2)
Br–C_β	1.86 (2)	1.86 (2)	1.86 (1)
C_α–C_m	1.37 (3)	1.38 (2)	1.39 (2)
C_m–C_{phe}	1.53 (3)	1.50 (2)	1.47 (7)
⟨C_{phe}–C_{phe}⟩	1.40 (3)		1.36 (4)
C_{phe}–C_{phe} (for rigid body)		1.395	
C_α–N–C_α	111 (2)	108 (1)	108 (1)
N–C_α–C_β	105 (1)	108 (1)	106 (1)
C_α–C_β–C_β	109 (1)	108 (1)	107.5 (7)
N–C_α–C_m	124 (1)	123 (1)	123 (1)

[a] C_α, C_β, C_m, and C_{phe} indicate respectively the α, β, meso, and phenyl carbon atoms of the macrocycles.

(16) (a) Hoard, J. L. In *Porphyrins and Metalloporphyrins*; Smith, K., Ed., Elsevier: Amsterdam, 1975; p 325. (b) Suh, M. P.; Swepston, P. N.; Ibers, J. A. *J. Am. Chem. Soc.* **1984**, *106*, 5164.
(17) Meyer, E. F., Jr. *Acta Crystallogr.* **1972**, *B28*, 2162.
(18) Cullen, D. L.; Meyer, E. F., Jr. *J. Am. Chem. Soc.* **1974**, *96*, 2095.
(19) Scheidt, W. R.; Lee, Y. J. *Struct. Bonding (Berlin)* **1987**, *64*, 1.

H_2TMOBP Br1--(o-CH_3) = 3.85, Br2--(o-CH_3) = 4.15, Br1--(o'-CH_3) = 4.15, and Br2--(o'-CH_3) = 3.85 Å and, for NiTMOBP, Br1--(o-CH_3) = 3.92, Br1--(o'-CH_3) = 4.17, Br2--(o-CH_3) = 4.25, and Br2--(o'-CH_3) = 3.79 Å. These distances correspond approximately to the sum of the van der Waals radii of Br (1.95 Å) and CH_3 (2.00 Å).[20] For NiTPFPOBP, all Br--F nonbonding separations are longer than 3.5 Å and exceed always the sum of the van der Waals radii of Br (1.95 Å) and F (1.35 Å).[20]

The individual NC_4 pyrrole rings are nearly planar in the three porphyrins. The largest deviations relative to the mean planes of these rings are at C4 of H_2TMOBP (0.06 (2) Å), C2 of NiTMOBP (0.06 (2) Å), and N21 in NiTPFPOBP (0.06 (2) Å). Br2 of H_2TMOBP lies approximately in the mean plane of the pyrrole ring, whereas Br1 is displaced 0.31 Å out of this mean plane away from the closest mesityl methyl (o'-CH_3). Reflecting the slightly increased distortion caused by the nickel insertion, both Br1 and Br2 are displaced from the pyrrole mean plane in NiTMOBP respectively 0.09 for Br1 and 0.24 Å for Br2. The average displacements are 0.15 Å for Br1 and 0.27 Å for Br2 in NiTPFPOBP. Adjacent pyrrole rings are tilted with respect to the porphyrin-core mean plane by 34.6 (8)° in H_2TMOBP, by 36.0 (5)° in NiTMOBP, and by angles ranging from 36.4 (8) to 41.4 (8)° in NiTPFPOBP. As expected, these tilts follow the trend of increased distortion in the nickel complexes. The dihedral angles between the phenyl ring planes and the mean porphyrin-core plane are 58.6 (6)° in H_2TMOBP, 58.3 (6)° in NiTMOBP, and 39.8 (6), 45.7 (5), 47.0 (5), and 48.1 (5)° in NiTPFPOBP.

The bond lengths and angles obtained for the octabrominated molecules are less accurate than those reported for most of the non-β-substituted, nearly planar porphyrins, for their metal derivatives, and for Zn(py)OMTPP and Zn(MeOH)OETPP.[5] Although the esd's of the bond lengths, bond angles, and thermal factors of the lighter atoms lying at the periphery are somewhat large, the possibility of significant improvement in the accuracy of the structural parameters is, at normal temperature, inherently limited by the presence in these molecules of eight heavy atoms. While detailed comparisons of bond lengths and bond angles with those present in nearly planar porphyrins and the saddle-shaped molecules Zn(py)OMTPP and Zn(MeOH)OETPP is therefore not possible, the important features of the molecular structures are readily apparent and meaningful discussion of the effects of β-bromine substituents is warranted.

The brominated porphyrins and metalloporphyrins described here exhibit the most severe S_4 saddle-shaped distortions of any porphyrin structure reported to date.[5d,19] Intermolecular nonbonding interactions do not appear to be responsible for these distortions. The porphyrin molecules, in these crystal structures, are arranged in layers. In H_2TMOBP and NiTMOBP, the shortest intermolecular nonbonding separations occur between the bromine atoms and methyl groups of adjacent molecules. All these separations are larger than 3.6 Å (Table S9, supplementary material). In NiTPFOBP, the lateral shift of the molecules is such that the nickel atom of one molecule overlaps on both sides of the macrocycle with bromine atoms of two neighboring porphyrins at Ni--Br distances of 3.41 and 3.51 Å. One short intermolecular nonbonding separation of 2.60 Å occurs between two fluorine atoms of molecules located in adjacent layers. All the other intermolecular contact distances have normal values (Table S9, supplementary material).

There is no evidence of π–π interactions between neighboring molecules in any of these structures. The phenyl rings of adjacent molecules do not overlap in any of the packing arrangements. Moreover, the porphyrin ring atoms are not in contact and the closest center to center approach distances of the pyrrole rings belonging to adjacent molecules are of 8.55 Å in H_2TMOBP, 8.64 Å in NiTMOBP, and 4.21 Å in NiTPFPOBP. The latter distance of 4.21 Å is quite small and could indicate the presence of weak π–π interactions.[19,21] However, although the mean planes of these pyrrole rings are parallel and separated only by 3.81 Å, these rings are shifted laterally and do not overlap directly.

In the bifacially hindered, nonbrominated tetramesitylporphyrin, the bulky o-Me groups form a molecular cavity on both sides of the macrocycle which prevents dimerization of iron(III) complexes by μ-oxo bond formation. The depth of the molecular cavity occurring on both sides of the ring can be defined as the vertical distance of the o- and o'-Me carbon atoms of the mesityl group above the 24-atom-core mean plane of the core.[22] These data are not known for the free base H_2TMP but for several metal complexes of this macrocycle, Zn(OH$_2$)TMP,[23] Ru(THF)(N$_2$)-TMP,[24] [CuTMP•]$^+$,[25] [Fe(1MeIm)$_2$TMP]$^+$, and [Fe(4-NMe$_2$py)$_2$TMP]$^+$.[26] In all these complexes except [Fe(4-NMe$_2$py)$_2$TMP]$^+$,[26] the porphyrinato core is almost planar and the 2- and 6-methyl substituents of the phenyl groups define, in each derivative, a symmetrical cavity. The average depths of these pockets have similar values; they range from 2.45 to 2.51 Å.[23,26] In contrast, in the ferric, low-spin, six-coordinate complex [Fe(4-NMe$_2$py)$_2$TMP]$^+$, the S_4 ruffling of the core leads to large variations in the position of the 2- and 6-methyl substituents. One class of methyl groups has an average perpendicular distance of 1.40 Å from the mean porphyrin plane, while the second class lies, on average, 3.25 Å away from this plane. A similar situation prevails in H_2TMOBP and NiTMOBP. Because of the S_4 saddle shape of the porphyrinato core, one class of methyl groups lies, on average, at 1.57 (H_2TMOBP) and 1.48 Å (NiTMOBP), while the second class is situated at 2.76 (H_2TMOBP) and 2.75 Å (NiTMOBP) above the mean porphyrin planes.

The o- and o'-F atoms of tetrakis(pentafluorophenyl)porphyrin H_2TPFPP offer only marginal steric hindrance to access to the central metal atom. Because of the doming of the macrocycles, the cavities on the inward and outward faces of the porphyrins in the iron(III) μ-oxo complex [(FeTPFPP)$_2$O] have slightly different sizes. The depth of the inward-facing cavity has been estimated to be close to 2.11 Å.[27] In NiTPFPOBP, the cavities present on both sides of the ring are virtually identical. The o- and o'-F pairs are located at average distances of 2.00 and 1.26 Å above the porphyrin-core mean plane.

The increased access to the metal oxo units in the peroxidase compound I models of these β-brominated porphyrins relative to their nonbrominated counterparts should have important consequences for their properties and selectivities as oxidation catalysts.[2e]

Acknowledgment. This work was supported by the Centre National de la Recherche Scientifique (UA 424 and UA 400) and NIH Grant ES03433 (A.G.). A.G. and R.W. thank NATO for a collaborative research grant. Financial support from the Université Louis Pasteur, Strasbourg, France, is also gratefully acknowledged.

Registry No. H_2TMOBP, 129006-48-0; NiTMOBP, 139944-27-7; ZnTMOBP, 128703-42-4; ZnTPFPP, 72076-08-5; ZnTPFOBP, 135693-27-5; H_2TPFPOBP, 139944-26-6; NiTPFPOBP, 139944-28-8; NiTPFPOBP·$^1/_2$CH$_2$Cl$_2$, 139944-29-9.

Supplementary Material Available: For H_2TMOBP, NiTMOBP, and NiTPFPOBP, listings of temperature factors for anisotropic atoms (Tables S1–S3), hydrogen atom positional parameters (Tables S4 and S5), complete bond distances (Tables S6–S8), shortest intermolecular contact distances (Table S9), and complete bond angles (Tables S10–S12) (18 pages); listings of observed and calculated structure factors amplitudes (×10) for all observed reflections (H_2TMOBP and NiTPFPOBP) or for all reflections (NiTMOBP) (Tables S13–S15) (20 pages). Ordering information is given on any current masthead page.

(20) Cotton, F. A.; Wilkinson, G. *Advanced Inorganic Chemistry*, 2nd ed.; Interscience Publishers: New York, 1966; p 105.

(21) Brennan, T. D.; Scheidt, W. R.; Shelnutt, J. A. *J. Am. Chem. Soc.* **1988**, *110*, 3919.

(22) Williamson, M. M.; Prosser-McCartha, C. M.; Mukundan, S., Jr.; Hill, C. L. *Inorg. Chem.* **1988**, *27*, 1061–1068.

(23) Song, H.; Scheidt, W. R. *Inorg. Chim. Acta* **1990**, *173*, 37–41.

(24) Camenzind, M. J.; James, B. R.; Dolphin, D.; Sparapany, J. W.; Ibers, J. A. *Inorg. Chem.* **1988**, *27*, 3054–3057.

(25) Song, H.; Reed, C. A.; Scheidt, W. R. *J. Am. Chem. Soc.* **1989**, *111*, 6865–6866.

(26) Safo, M. K.; Gupta, G. P.; Walker, F. A.; Scheidt, W. R. *J. Am. Chem. Soc.* **1991**, *113*, 5499–5510.

(27) Gold, A.; Jayaraj, K.; Doppelt, P.; Fischer, J.; Weiss, R. *Inorg. Chim. Acta* **1988**, *150*, 177–181.